Nonmesomorphic Solute−Mesomorphic Solvent Interactions Studies. 3. A Unified Approach To Probe Liquid Crystalline Order by Electron Spin Resonance Spectroscopy

M. A. Morsy,* J. S. Hwang, and G. A. Oweimreen

Department of Chemistry, King Fahd University of Petroleum & Minerals, Dhahran 31261, Saudi Arabia

Received: August 15, 1996; In Final Form: November 15, 1996[⊗]

This paper reports values for the **A** and **g** magnetic tensor components for PD-Tempone in the rigid limit of the *n*-pentyl (5CB), *n*-hexyl (6CB), *n*-heptyl (7CB), and *n*-octyl (8CB) cyanobiphenyl liquid crystals and for Tempo-Palmitate in the rigid limit of 5CB and 6CB. A unified approach based on introducing a factor into the "distortion theory" expression for obtaining probe order parameters S_{ii} is successfully tested. The sign and value of this factor give the probability of alignment of the *i*th axis of the probe along the applied magnetic field.

Introduction

It is now established[1−7] that the macroscopic alignment of mesomorphic phases may be investigated by electron spin resonance spectroscopy (ESR) using radical dopants as probes. Researchers endeavored to synthesize probes with structures that mimic the structure of the liquid crystalline molecules as closely as possible. For example, Ferruti *et al.*[3] synthesized such a probe and used its N^{14}-hyperfine patterns and *g*-factor shifts to determine its alignment with respect to the liquid crystalline solvent. Another such probe was synthesized and used by Luckhurst and Yeates[8] in an ESR experiment that involved the variation of the angle between the applied magnetic field and the director in the mesophases of various nematogens to determine their order parameters. The assumption that these probes are axially symmetric and the fact that the second-rank tensor for the order parameter is traceless led Luckhurst and his co-workers[2,8,9] and Ferruti *et al.*[3] to conclude that S_{22} and S_{33}, the order parameters perpendicular to the magnetic field, are equal to $-{}^1/_2S_{11}$, where S_{11} is the order parameter along the magnetic field.

Recent studies[10,11] using PD-Tempone (PDT) and Tempo-Palmitate (PT) probes show that a probe with a structure similar to that of the liquid crystalline solvent may not necessarily be the most suitable probe for investigating that solvent. In addition it has been found that PDT and TP mainly rotate, respectively, along their *y* and *x* molecular rotational axes. These findings and the fact that the assumption that the probe is axially symmetric is rarely fulfilled led us to seek a more general approach to determine the alignment of the probe with respect to the magnetic field. The proposed approach incorporates a factor into the "distortion theory" expression[9] for the ordering matrix.

We have successfully tested this approach relying on measurements of the **A** and **g** magnetic tensor components for PDT in the rigid limit of the *n*-pentyl (5CB), *n*-hexyl (6CB), *n*-heptyl (7CB), and *n*-octyl (8CB) cyanobiphenyl liquid crystals and for TP in the rigid limit of 5CB and 6CB and our previously measured[10,11] hyperfine spacing, *a*, and *g*-factor values in the different phases of these systems. Interpretations for the sign and value of the above mentioned factor are proposed. In addition, our results demonstrate that S_{11} and S_{22} reflect the ordering of the probe in a solvent whereas S_{33} reflects solvent order.

Finally, the use of this approach on data taken from Ferruti *et al.*[3] for *p*,*p*′-(hexyloxy)azoxybenzene (PAHB) and *p*-phenetylazophenylhexanoate led to the same order parameters obtained by them without making their assumptions regarding probe symmetry. Where the approach by Ferruti *et al.*[3] failed to show that S_{11} values obtained from Δa and Δg expressions (eqs 4, ref 3) were identical, our approach succeeded.

Theoretical Considerations

The spin Hamiltonian describing the ESR of a nitroxide radical in a nematogenic solvent[9] is

$$H = (g + \Delta g)\beta H_0 S_z + (a + \Delta a)hI_z S_z \qquad (1)$$

where *g* and *a* are the isotropic invariants of the *g*-factor tensor ($={}^1/_3(g_x + g_y + g_z)$) and the hyperfine tensor ($={}^1/_3(A_x + A_y + A_z)$) of the electron with the ^{14}N nucleus, respectively. The tensors cannot be calculated directly, but they can be extracted from the information in the ESR spectrum of the spin probe at the rigid limit. Δg and Δa are the shifts in *g* and *a* respectively, resulting from the ordering at temperatures below the isotropic-to-nematic (I → N) transition temperature (t_{IN}) and are given by[2]

$$\Delta g = {}^2/_3\sum_{\alpha,\beta} S_{\alpha\beta} g_{\alpha\beta} \qquad (2)$$

$$\Delta a = {}^2/_3\sum_{\alpha,\beta} S_{\alpha\beta} A_{\alpha\beta} \qquad (3)$$

where $A_{\alpha\beta}$, $g_{\alpha\beta}$, and $S_{\alpha\beta}$ are, respectively, the second-rank anisotropic hyperfine spacing, g-factor, and ordering matrix tensors with α and β denoting Cartesian axes set in the probe molecule. $S_{\alpha\beta}$ are the elements of the ordering matrix **S** defined by Luckhurst[2] and originally introduced by Saupe[12] to describe the extent of solute alignment in a liquid crystal. The average orientational orders of the spin probe in the mesophase reduce the number of the independent elements in the ordering matrix **S** into five[3] thus

$$\Delta g = {}^2/_3(S_{11}g_{xx} + S_{22}g_{yy} + S_{33}g_{zz}) \qquad (4)$$

$$\Delta a = {}^2/_3(S_{11}a_{xx} + S_{22}a_{yy} + S_{33}a_{zz}) \qquad (5)$$

For the special case of a probe molecule cylindrically symmetric about its *x*-axis, the traceless property of the diagonal elements

[⊗] Abstract published in *Advance ACS Abstracts,* February 15, 1997.

S1089-5647(96)02514-X CCC: $14.00

of the ordering matrix **S** gives $S_{22} = S_{33} = -{}^1/_2 S_{11}$ and eqs 4 and 5 become[3]

$$\Delta g = {}^1/_3(2g_{xx} - g_{yy} - g_{zz})S_{11} \quad (6)$$

$$\Delta a = {}^1/_3(2a_{xx} - a_{yy} - a_{zz})S_{11} \quad (7)$$

The requirement of cylindrical symmetry is very difficult to achieve experimentally, and the relation $S_{22} = S_{33} = -{}^1/_2 S_{11}$ will invariably represent an approximation of the true situation. The difficulty in synthesizing probes that approach such cylindrical symmetry and our finding[11] that such probes are not necessarily more suitable for studying liquid crystalline phases than the commonly available probes (e.g. PD-Tempone or even the cheaper Tempone) led us to modify earlier findings by satisfying the traceless property of the ordering matrix through the introduction of an *f*-factor. Thus for a molecule rotating about its *x*-axis the traceless property of the ordering matrix is satisfied by

$$S_{22} = -f_x S_{11} \quad (8)$$

$$S_{33} = -(1 - f_x)S_{11} \quad (9)$$

where for the special case of a cylindrically symmetric molecule $f_x = 0.5$. Substituting the S_{22} and S_{33} expressions from eqs 8 and 9 into the Δg and Δa expressions in eqs 4 and 5 and solving for f_x gives

$$f_x = \frac{\Delta g(a_z - a_x) + \Delta a(g_x - g_z)}{\Delta g(a_z - a_y) + \Delta a(g_y - g_z)} \quad (10)$$

For probes like PDT which rotate about their *y*-axis, one can derive another expression for f_y using the following traceless property of the ordering matrix

$$S_{11} = -f_y S_{22} \quad (11)$$

$$S_{33} = -(1 - f_y)S_{22} \quad (12)$$

where $f_y = 0.5$ for a molecule which rotates about its *y*-axis and is cylindrically symmetric about its *y*-axis. It turns out that the expression obtained for f_y is the reciprocal of the right-hand side of eq 10.

Experimental Section

The hyperfine spacing, *a*, and the *g*-factors for PDT in 5CB, 6CB, 7CB, and 8CB and TP in 5CB and 6CB have been previously reported.[10,11] All information relating to these systems such as materials, sample preparation, apparatus, and data collection is given in refs 10 and 11.

Since the PDT spectra in the frozen nematogenic liquid crystalline systems were found to be independent of whether the sample is amorphous or glassy,[1] the six liquid crystalline systems studied were immersed in liquid nitrogen to form rigid glasses at about 77 K. Experimental (continuous lines) and simulated (dashed lines) rigid limit ESR spectra for the PDT/5CB and TP/5CB systems are shown in Figure 1. The agreement between experimental and simulated spectra for all the systems studied is the same or better than the representative spectra in Figure 1. The resolution in the central region of the PDT/5CB system (Figure 1a) is absent from the same region for the TP/5CB (Figure 1b) system. This difference between PDT and TP probes might be due to their rotations about different molecular axes, namely their *y* and *x*-axes, respectively.[10,11] Another reason suggested[1,13] for this difference is the inhomogeneous broadening due to unresolved proton hyperfine structure in TP.

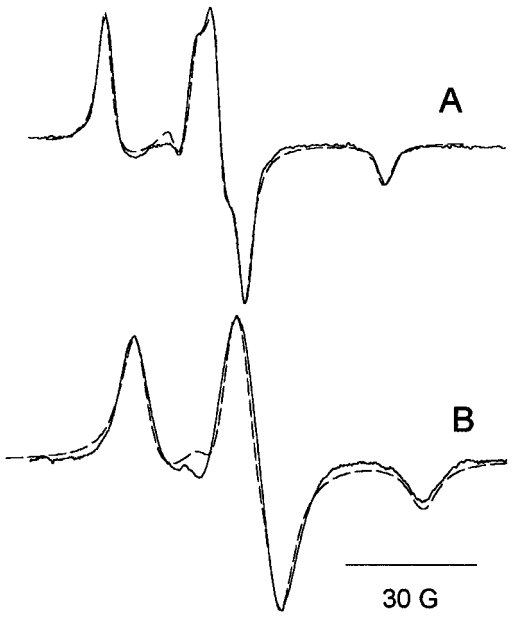

Figure 1. Experimental (continuous lines) and simulated (dashed lines) rigid limit ESR spectra for (a) PD-Tempone (PDT) and (b) Tempo-Palmitate (TP) in 5CB at 77 K.

The rigid limit simulations of all the studied systems were performed using the general method of Lefebre and Maruani[14] adapted to nitroxide radicals in liquid crystalline media by Polnaszek.[15] The simulation employs Simpson's numerical integration over θ in 45 intervals and over φ in 25 intervals and a liquid crystal potential value between 0.245−0.380. The parameters of the **A** and **g** tensors which gave the best fit for all the systems are given in Table 1. The parameters a_z and g_z correspond to the midpoint of the two extrema. a_z is half the difference between the field values at the two extrema, and g_z is calculated from the frequency and the field at the midpoint between the two extrema. The tensor parameters a_x, a_y, g_x, and g_y and the line width are varied to fit the experimental spectrum until the line shape of the central portion is simulated. The Lorentzian line shape gave the best overall fit.

Results and Discussion

Hyperfine Spacing and *g*-Factor Shifts. The *a*-values for a nitroxide radical probing the isotropic phases of homologous liquid crystal series are equal and constant down to their I → N transition temperatures. On the other hand, the *g*-factors for such probes in the isotropic phases of homologous liquid crystals increase with decrease in temperature down to the onset of the I → N transition temperature, t_{IN}, where they exhibit an odd−even effect.[10,11] The variation of *g* with *t* is illustrated by the closed circles in parts A1 and B1 of Figure 2 for PDT and TP, respectively, in 5CB. Similar results were obtained for PDT and TP in 6CB and for PDT in 7CB and 8CB. Postulating that this dependence of *g* on temperature persists below t_{IN} necessitates a correction for the temperature effect whenever an analysis of the effect of nematogenic ordering on *g* is undertaken. As the *g* versus *t* behavior in the isotropic phase varies with the nature of the probe (Figure 2A1,2B1) different correction procedures, outlined in the two following paragraphs, were used.

For TP in the isotropic phases of 5CB and 6CB, the variation of *g* with *t* was found to be virtually linear with a slope of -1.160×10^{-5} °C^{-1} up to the onset of the I → N transition

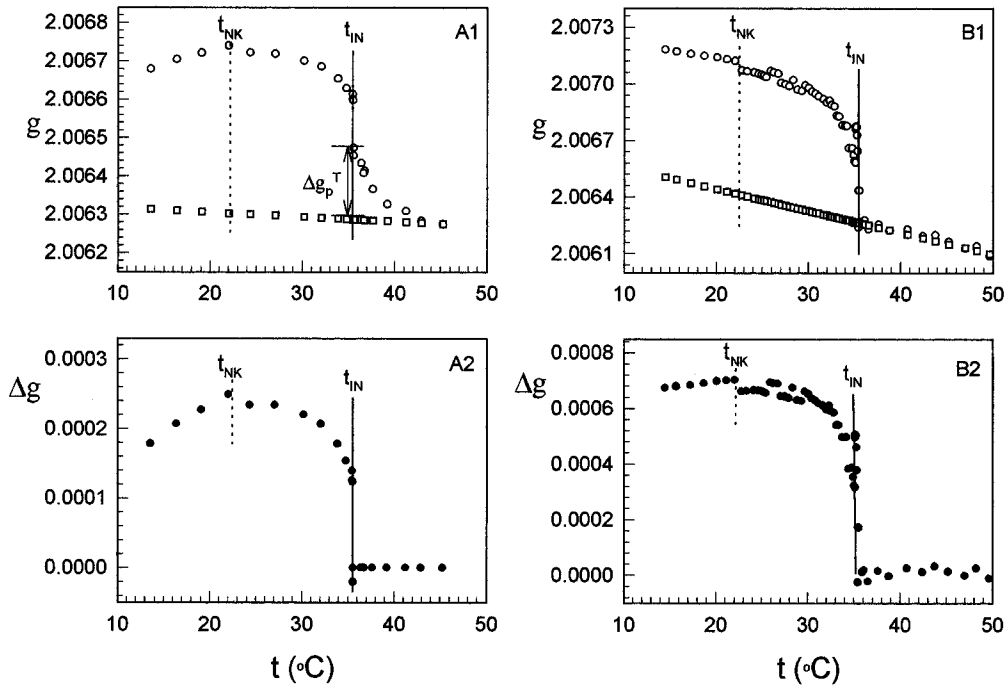

Figure 2. Observed *g*-factors (open circles) and order independent calculated *g*-factors (open squares) at different temperatures for (A1) PDT in 5CB and (B1) TP in 5CB and the change in the *g*-factors at different temperatures due to the reorientational order for (A2) PDT in 5CB and (B2) TP in 5CB. Vertical solid lines are drawn at the isotropic-to-nematic transition temperatures. Dotted vertical lines are drawn at the nematic-to-crystal transition temperatures on the basis of the transition temperatures reported by the manufacturer (BDH).

TABLE 1: Magnetic Parameters for PDT and TP in Alkylcyanobiphenyl Liquid Crystalline Solvents

probe	solvents	g_x	g_y	g_z	$\langle g \rangle$	a_x	a_y	a_z	$\langle a \rangle$
PDT	5CB	2.009 95	2.006 70	2.002 68	2.006 44	4.95	5.30	33.81	14.69
	6CB	2.009 80	2.007 20	2.002 97	2.006 66	4.95	5.30	33.81	14.69
	7CB	2.009 90	2.006 64	2.002 46	2.006 33	4.95	5.30	33.81	14.69
	8CB	2.009 78	2.007 18	2.002 81	2.006 59	4.95	5.30	33.81	14.69
TP	5CB	2.009 75	2.007 25	2.002 65	2.006 53	5.90	6.00	34.65	15.52
	6CB	2.009 78	2.007 63	2.002 73	2.006 71	5.90	6.00	34.60	15.50

where a sharp increase in g occurs. The intercepts of the g versus t fits were 2.006 67 in 5CB and 2.006 90 in 6CB. This finding suggests that the slope depends on the type of probe while the intercept reflects solvent structure.[11] Assuming that the linear dependence of the g-factor on temperature in the isotropic phase persists in the nematic phase, g-factor shifts (Δg) reflecting ordering due to the nematic structure only are obtained from

$$\Delta g = g_N - g_{I,v} \tag{13}$$

where g_N is the experimental g-factor value at a temperature in the nematic phase and $g_{I,v}$ is the g-factor for a "virtual" isotropic phase obtained from an extrapolation of the above mentioned fit to that temperature. The variation of Δg with temperatures is shown for TP in 5CB in Figure 2B2 as a representative example.

For PDT in the isotropic phases of 5CB, 6CB, 7CB, and 8CB the variation of g with t is less simple. Although a large number of data over wide temperature ranges were collected in the isotropic phases of these systems,[11] the linear variation of g with t was clearly distinguishable only in the PDT/6CB system (intercept = 2.006 62 and slope = -1.202×10^{-6} °C^{-1}). Prior to the I → N transition in all these systems (about 3 °C for 6CB and as high as 15 °C for 7CB), the increase in g with decrease in temperature deviated from linearity. Since, as has been mentioned, in the TP/5CB and TP/6CB systems the g versus t lines have the same slope (i.e., they reflect the probe rather than the solvent), one would expect that at varying temperatures above the isotropic to nematic transition linear g versus t plots of identical slopes would be found for the PDT/RCB systems. On the basis of this argument the linear variations of g with t in the isotropic phases of the PDT/5CB, PDT/7CB, and PDT/8CB systems were obtained by passing a line of slope equal to -1.202×10^{-6} °C^{-1} through the point(s) where such linearity was reached/approached. The intercepts of these lines exhibited an odd−even effect reminiscent of that previously encountered[11] with the g-values of these systems at the onset and completion of the I → N transition (see Figure 3). The observed pretransitional deviation from linearity Δg_p attributable to cluster formation is at its maximum value Δg_p^T at the I → N transition which is given by

$$\Delta g_p^T = g_I^T - g_{I,v}^T \tag{14}$$

where g_I^T is the value of g at the onset of the I → N transition and $g_{I,v}^T$ is the value of $g_{I,v}$ at the I → N transition temperature. Thus at any other temperature in the nematic phase the change in the g-factor shift (Δg) reflecting ordering due to the nematic structure only is obtained from

$$\Delta g = g_N - \Delta g_p^T - g_{I,v} \tag{15}$$

The variation of Δg with temperatures is shown for PDT in 5CB in Figure 2A2 as a representative example. Since Δg reflects ordering due to nematic structure, only its value in the isotropic phase is fixed at zero.

The shifts in the hyperfine spacing a and g-factor values Δa and Δg, respectively, for PDT in the nematic phases (and

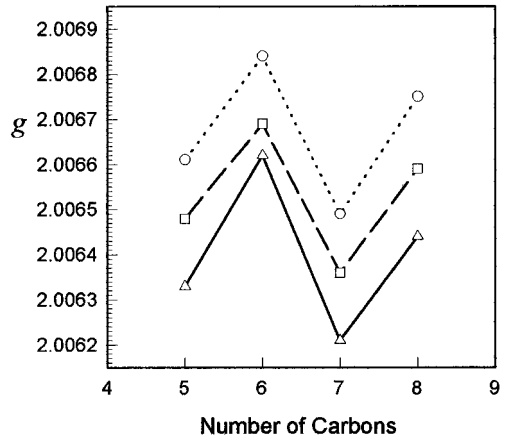

Figure 3. (○) and (□) *g*-factors at the onsets of the nematic phase on cooling and the isotropic phase on heating, respectively, for PDT versus the number of carbons in the alkyl tail of the 5CB, 6CB, 7CB, and 8CB solvent molecules. (△) intercepts at $t = 0$ °C of linear fits for the *g*-factor versus temperature in the isotropic phases of the same systems.

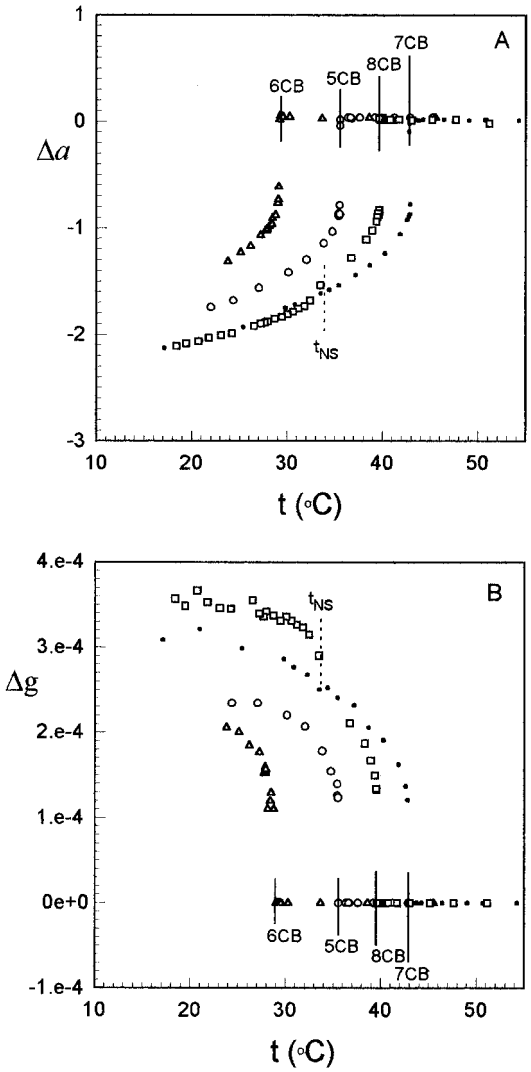

Figure 4. Shifts in (A) the hyperfine spacing *a* and (B) the *g*-factor for PDT in 5CB, 6CB, 7CB, and 8CB at different temperatures. Vertical solid lines are drawn at the isotropic-to-nematic transition temperatures. Dotted vertical lines are drawn at the nematic-to-smectic temperature.

smectic phase in the case of 8CB) of all the studied liquid crystals are given in Figure 4A,B. Similar data have been observed for the TP in 5CB (Figure 2B2) and 6CB. The opposite sign of Δa and Δg are expected.[3] That a discontinuity

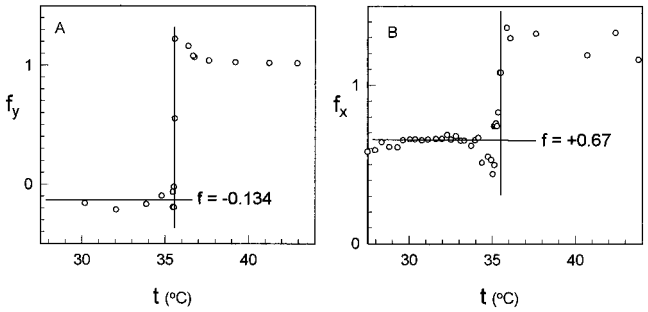

Figure 5. Variation of the *f*-factor with temperature for (A) PDT and (B) TP in 5CB. Vertical lines are drawn at the isotropic-to-nematic transition temperatures.

is observed for Δa and more clearly for Δg at the weak first-order nematic-to-smectic transition t_{NS} is a clear indication that these shifts are a measure of order within a phase.

***f*$_i$-Values and Order Calculations.** The odd−even effect in the *g*-factors at the onset of either the nematic or isotropic phase[11] and in the intercepts at $t = 0$ °C of the linear fits of *g* versus *t* in the isotropic phases (Figure 3) and the differences between the a_{iso} values for PDT and TP in the same solvent led us to refrain from using rigid limit parameters obtained for one liquid crystal system on another as has been done in previous studies.[1,10] In this study each system is analyzed using its own rigid limit parameters (see Table 1). The rigid limit parameters and the Δa and Δg values are substituted into eq 10 to obtain the factors f_x and f_y for TP and PDT, respectively. Once f_x is known eqs 8, 9, 4, and 5 are solved to give the parallel orientational order tensor S_{11} for TP either from the Δa equation or the Δg equation; thus

$$\Delta a = {}^2/_3[(a_x - a_z) + f_x(a_z - a_y)]S_{11} \quad (16)$$

$$\Delta g = {}^2/_3[(g_x - g_z) + f_x(g_z - g_y)]S_{11} \quad (17)$$

Similarly from f_y and eqs 11, 12, 4, and 5 the parallel orientational order tensor S_{22} for PDT is obtained from

$$\Delta a = {}^2/_3[(a_y - a_z) + f_y(a_z - a_x)]S_{22} \quad (18)$$

$$\Delta g = {}^2/_3[(g_y - g_z) + f_y(g_z - g_x)]S_{22} \quad (19)$$

Parts A and B of Figure 5 show the variation of *f* with temperature for PDT and TP, respectively, in 5CB. More or less the same values of f_y (≈−0.134) and values of f_x (≈+0.67) were obtained for the nematic phases probed with PDT and TP, respectively, in the different liquid crystalline solvents. These results are explained in the following paragraphs.

If the alkyl tail on the TP probe was in an all-trans conformation as shown in Scheme 1, TP would be cylindrically symmetric and would have an f_x value of +0.5. Clearly the constraint on the alkyl tail of TP by the nematogenic order is not enough to achieve a complete all-trans conformation and the existence of other conformations and f_x value deviates from +0.5. Thus the f_x obtained by us can be viewed as a measure of the deviation of the TP molecule from cylindrical symmetry. Moreover, the positive sign of f_x indicates that the *x*-axis, which is the axis of rotation of the probe molecule, lies along the applied magnetic field.

On the other hand, the structure of PDT (Scheme 1) shows it will never be cylindrically symmetric about its *y* rotational axis;[10] thus f_y will not be +0.5. The sign for f_y indicates that a fraction of the PDT radicals rotate about their *x*-axis. From the traceless property of the order tensor matrix it can be shown

SCHEME 1

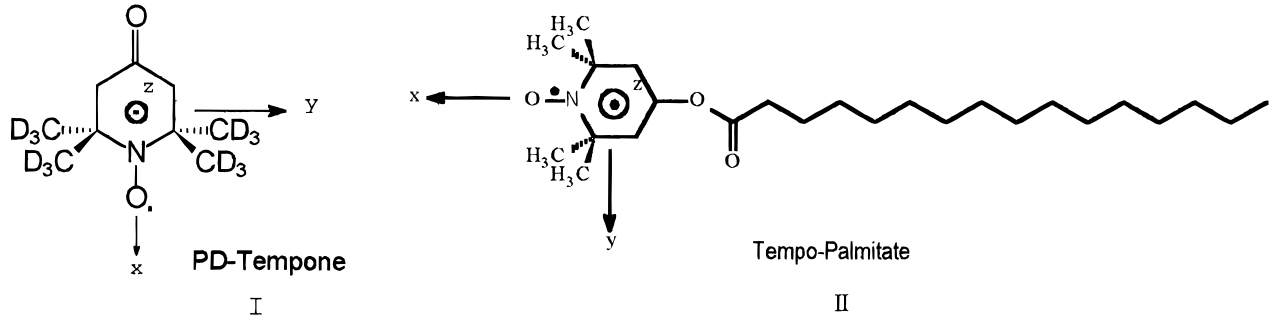

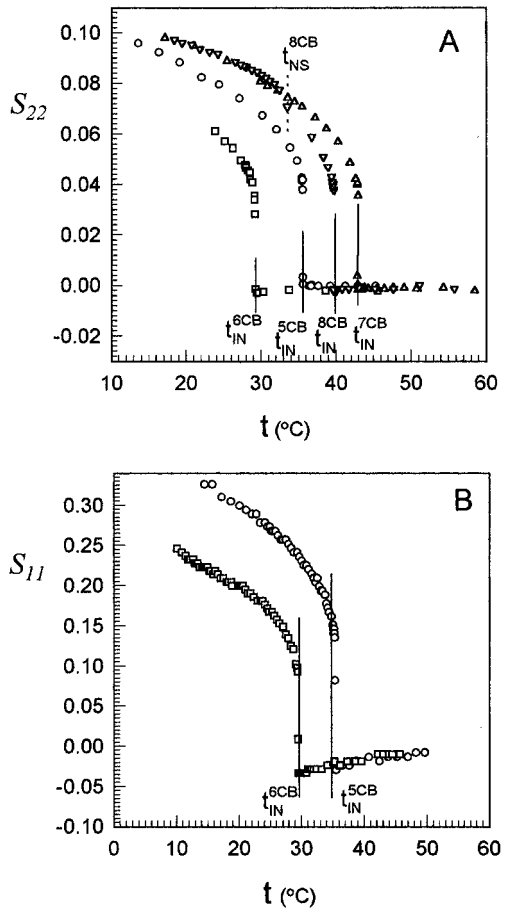

Figure 6. Values of the parallel orientational order tensor (A) S_{22} for PDT in 5CB, 6CB, 7CB, and 8CB and (B) S_{11} for TP in 5CB and 6CB at the experimental temperatures. Vertical solid lines are drawn at the isotropic-to nematic transition temperatures. Dotted vertical line is drawn at the nematic-to-smectic transition temperature.

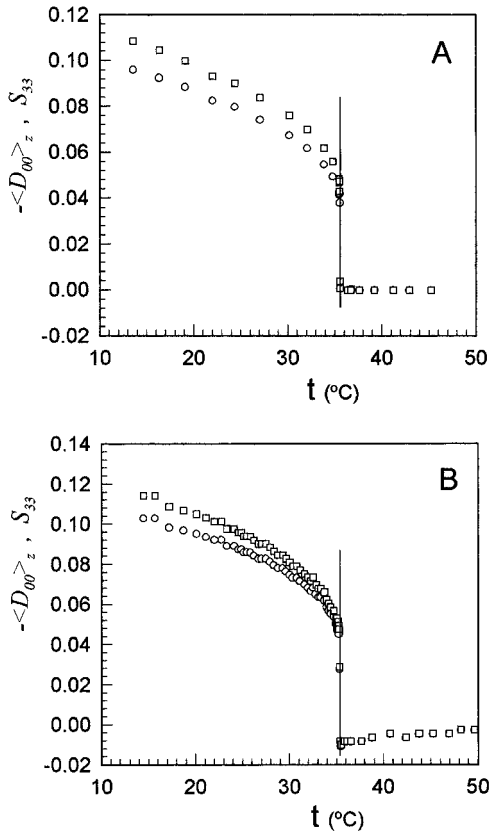

Figure 7. Variation of $\langle D_{00}^2 \rangle_z$ (○) and S_{33} (□) with temperature for (A) PDT and (B) TP in 5CB. Vertical lines are drawn at the isotropic-to-nematic transition temperatures.

that the percent of probes rotating about the *x*-axis is given by $100S_{11}/(S_{11} + S_{22})$; thus, the f_y value obtained for PDT shows that about 12% of the PDT radicals rotate about the *x*-axis. The axis of rotation of a probe is along the applied magnetic field irrespective of whether it is a *y*- or an *x*-axis; i.e., a probe rotating about its *x*-axis has its *x*-axis along the applied magnetic field, and one rotating about its *y*-axis has its *y*-axis along magnetic field. This is in harmony with earlier results from line width analysis[10] which shows that PDT radicals rotate mainly about their *y*-axis.

Using either eq 18 or eq 19 the parallel orientational order tensor values, S_{22}, were obtained for PDT at all the experimental temperatures in 5CB, 6CB, 7CB, and 8CB, and the results are given in Figure 6A. A small change in order is detected close to the nematic-to-smectic transition temperature t_{NS} of 8CB. The absence of an abrupt change in S_{22} at the temperatures corresponding to the nematic-to-crystal transitions (or smectic-to-crystal transition for 8CB) indicates that solidification has not taken place and that the liquid crystals are in a supercooled state. In a similar manner eq 16 or eq 17 leads to plots of the parallel orientational order tensor for TP, S_{11}, at different temperatures in 5CB and 6CB (Figure 6B).

The Significance of the Order Tensor Values. Parts B and A of Figure 6, respectively, show that the S_{11} values for TP in 5CB (or 6CB) are very different from the S_{22} values for PDT in 5CB (or 6CB), although in either case the probe axis of rotation is parallel to the applied magnetic field. Clearly S_{11} and S_{22} reflect the ordering of the probes within an ordered phase. On the other hand, the perpendicular orientational order parameters, S_{33}, obtained for PDT and TP in 5CB (parts A and B of Figure 7, respectively) are comparable; i.e., they are practically independent of the axes of rotation. This suggests that S_{33} reflects mainly the ordering of the studied solvent.

S_{33} corresponds to Saupe's ordering tensor O_{zz},[16] which in turn corresponds to Freed's solute ordering parameter $\langle D_{00}^2 \rangle_z^1$

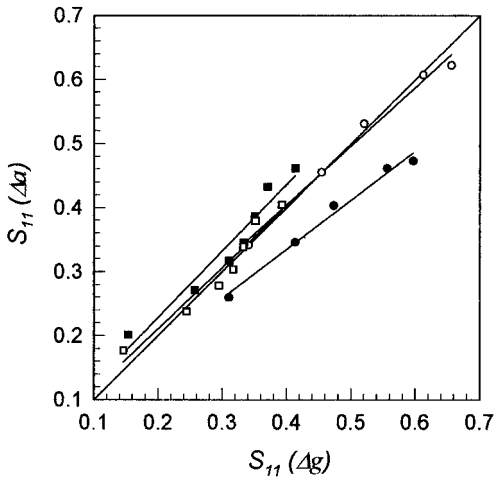

Figure 8. $S_{11}(\Delta a)$ versus $S_{11}(\Delta g)$ for 2,2,6,6-tetramethyl-4-(p-octyloxy)benzoylaminopiperidin-1-oxyl in *p,p′*-(hexyloxy)azoxybenzene (○ and ●) and *p*-phenylazophenylhexanoate (□ and ■). (○) and (□) refer to $S_{11}(\Delta a)$ versus $S_{11}(\Delta g)$ values calculated, respectively, from eqs 16 and 17 in the text. (●) and (■) refer to $S_{11}(\Delta a)$ versus $S_{11}(\Delta g)$ values calculated from eqs 4 in ref 3.

which is given by

$$\langle D^2_{00}\rangle_z = \frac{(\langle a\rangle - a)(g_x - g_y) - (\langle g\rangle - g)(a_x - a_y)}{(a_z - a)(g_x - g_y) - (g_z - g)(a_x - a_y)} \quad (20)$$

where $(\langle a\rangle - a)$ and $(\langle g\rangle - g)$ correspond to $-\Delta a$ and $-\Delta g$, respectively, in this paper. The $\langle D^2_{00}\rangle_z$ calculated using eq 20 (eq 2.26a in ref 1) at all the experimental temperatures in the PDT/5CB (Figure 7A) and TP/5CB (Figure 7B) systems are slightly lower than the corresponding S_{33} values. The proximity between the S_{33} values for the TP/5CB and PDT/5CB systems is better (by a factor of about 0.5) than that for $\langle D^2_{00}\rangle_z$ for the same systems (Figure 7A,B). This suggests that the S_{33} values are better than $\langle D^2_{00}\rangle_z$ values at reflecting solvent order and may be preferred for transformation[1,10] to the Maier−Saupe potential lambda, λ.

Using a probe with a structure similar to that of liquid crystal molecules and assuming it has $S_{22} = S_{33} = -0.5S_{11}$, Ferruti *et al.*[3] find that the S_{11} values calculated from eq 16 and S_{11} values calculated from eq 17 are, contrary to their expectation, not linearly related. Using our approach, which is not restricted to an axially symmetric probe, on Ferruti's data that deviated most from linearity, we verified (see Figure 8) the identity of the S_{11} values from eqs 16 and 17.

Conclusion

Ways for correcting the change in the *g*-factor of a probe due to nematic ordering, Δg, for pretransitional ordering and/or temperature dependence have been proposed. The change in the hyperfine spacing due to nematic ordering values, Δa, corrected Δg values, and the parameters of the **A** and **g** tensors (obtained for our probe/liquid crystal systems from simulations that fit results of rigid limit measurements) were used in the "distortion theory" expression modified for any probe, irrespective of its symmetry, by the introduction of a factor *f*. The resulting equations fit previously obtained data without invoking any assumption regarding probe symmetry. The sign and value obtained for the *f*-factor for a probe carry information about the probability of its alignment along the applied magnetic field.

Acknowledgment. We thank King Fahd University of Petroleum & Minerals for support of this work.

References and Notes

(1) Polnaszek, C. F.; Freed, J. H. *J. Phys. Chem.* **1975**, *79*, 2283.
(2) Luckhurst, G. R. In *Liquid Crystals and Plastic Crystals*; Gray, G. W. Winsor, P. A., Eds., Ellis Horwood: New York, 1975; Vol. 2, Chapter 7.
(3) Ferruti, P.; Gill, D.; Harpold, M. A.; Klein, M. P. *J. Chem. Phys.* **1969**, *50*, 4545.
(4) Oweimreen, G. A.; Hwang, J. S. *Liq. Cryst.* **1989**, *5*, 585.
(5) Luckhurst, G. R.; Sanson, A. *Mol. Phys.* **1972**, *24*, 1297.
(6) Luckhurst, G. R.; Setaka, M.; Zannoni, C. *Mol. Phys.* **1974**, *28*, 49.
(7) Nayeem, A.; Freed J. H. *J. Phys. Chem.* **1989**, *93*, 6539.
(8) Luckhurst, G. R.; Yeates, R. N. *Mol. Cryst. Liq. Cryst.* **1976**, 996.
(9) Luckhurst, G. R. *Mol. Cryst.* **1967**, *2*, 363.
(10) Hwang, J. S.; Morsy, M. A.; Oweimreen, G. A. *J. Phys. Chem.* **1994**, *98*, 9056.
(11) Morsy, M. A.; Oweimreen, G. A.; Hwang, J. S. *J. Phys. Chem.* **1996**, *100*, 8533.
(12) Saupe, A. *Angew. Chem., Int. Ed. Engl.* **1968**, *7*, 97. Saupe, A.; Englert, G.; Povh, A. *Adv. Chem. Ser.* **1967**, *63*, 51. Saupe, A. *Z. Naturforsch.* **1964**, *199*, 161.
(13) Hwang, J. S.; Pollet, P.; Saleem, M. M. *J. Chem. Phys.* **1986**, *84*, 577.
(14) Lefebre, L.; Maruani, *Mol. Phys.* **1968**, *14*, 349.
(15) Polnaszek, C. F. Ph.D. Thesis, Cornell University, 1975.
(16) Maier, W.; Saupe, A. *Z. Naturforsch. A* **1958**, *13*, 564.